The background of the cover features a close-up photograph of a 3D printed metal mesh structure, likely a filter or waveguide component, mounted on a precision mechanical assembly. The lighting is dramatic, highlighting the intricate details of the mesh and the metallic surfaces of the machinery.

WHITE PAPER

**APPLICATIONS GUIDE TO 3D PRINTED LOW-LOSS
DIELECTRIC STRUCTURES ADDRESSING
MICROWAVE/MMWAVE CHALLENGES**



TABLE OF CONTENTS

- 1** INTRODUCTION
- 2** DIELECTRIC RESONATOR ANTENNAS (DRAS) AND DIELECTRIC REFLECTARRAY ANTENNA (DRA) [5]-[15]
- 3** DIELECTRIC BLADE ANTENNAS [8], [10], [16]-[19]
- 4** REPLACEMENT PROCESS FOR DIELECTRIC FOAMS IN MICROWAVE/MILLIMETER-WAVE ANTENNA AND RADOME APPLICATIONS [20]-[24]
- 5** DIELECTRIC WAVEGUIDES FOR UPPER MILLIMETER-WAVE & THZ APPLICATIONS INCLUDING SUBSTRATE INTEGRATED WAVEGUIDE COMPONENTS [25]-[31]
- 6** CUSTOM WAVEGUIDE AND TAILORED WAVEGUIDE PROPAGATION CHARACTERISTICS WITH DIELECTRIC LOADS INCLUDING WAVEGUIDE FILTERS [32], [27]-[31], [33]-[36]
- 7** FLAT/PANEL ANTENNAS/LENSES FOR SATELLITE AND UNMANNED VEHICLE (LOW-PROFILE) & COLLAPSIBLE ANTENNA ARRAY/ SYSTEM [37]-[42]
- 8** CONCLUSION



1

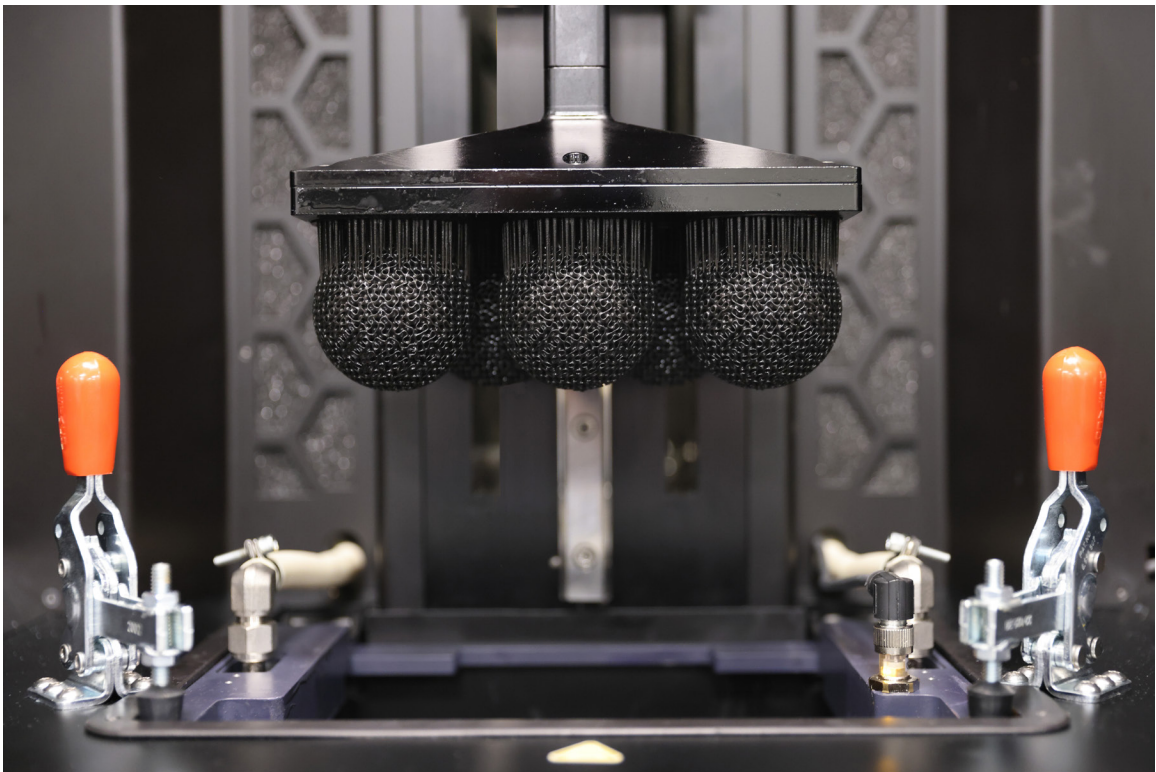
INTRODUCTION

Dielectric materials are both electrically and mechanically significant in virtually all Microwave/millimeter-wave (mmWave) components and devices. For nearly all cases with the exception of integrated circuit (IC) technologies, Microwave/mmWave dielectrics have historically been fabricated from planar sheets, traditionally machined, or molded. With planar dielectric sheets, such as PCB laminates, making complex 3D dielectric or mixed dielectric/conductive structures requires layering or complicated 3D assembly that suffer from tolerance and repeatability challenges. Though traditional machining, such as CNC milling/lathing, can result in extremely tight tolerances and small feature sizes, subtractive manufacturing methods such as these have limited degrees of freedom, especially in concern to internal cavities, without stacking of machined parts. Furthermore, creating molded dielectric parts requires the high expense and long lead-time of having a mold fabricated and is generally only justified if many thousands of the same part will be manufactured. These legacy approaches to manufacturing Microwave/mmWave dielectrics can also suffer from material property limitations, especially with low-loss and low-dielectric constant material choices. Historically this has also been the case with additive manufacturing methods, such as fused deposition modeling (FDM), stereolithography (SLA), or digital light processing (DLP) 3D printing. There are a wide range of plastic and resin materials that exhibit good printability profiles, but ultimately lack the necessary low-loss (loss tangent, or $\tan \Delta$) and low dielectric constant properties for Microwave/mmWave applications.

Recently, 3D printable resins with desirable Microwave/mmWave characteristics and 3D printing processes have been established that enable 3D DLP manufacturing of both low-loss and low-dielectric constant material that are viable for prototyping and production scale manufacturing [1]–[4]. These new 3D printing processes can yield structures with 10s of microns of resolution (100s of microns feature sizes/wall thickness) with a base material dielectric constant of $2.8\epsilon_r$ for a polymer-based dielectric, and base dielectric constant of $8\epsilon_r$ for a high purity Alumina (HP-A) ceramic material. Using such a 3D printed polymer resin process, a lattice dielectric structure with good mechanical features can be designed and fabricated with an effective dielectric range from as high as $2.8\epsilon_r$ to as low as $1.15\epsilon_r$. The lowest achievable effective relative permittivity depends on the design of hollow to filled spaces and feature sizes.



The feature size limitations of this process are a result of what is necessary for the finished part to maintain structural integrity during the printing, post processing, and use case environmental scenarios. Though the DLP print bed size effectively limits the size of a single printed dielectric structure, a much larger structure could be designed from parts that are precision indexed to assemble into that larger structure. There are also potential processes being developed to fully metallize, or even selectively metallize the resulting dielectric structures. Hence, this new dielectric fabrication process unleashes an unprecedented degree of freedom for manufacturing high performance Microwave/mmWave dielectric structures and potentially even fabricating complete antennas, lenses, waveguide, filters, or other components.



3D printed GRIN (Graded Refractive Index) lenses on the FLUX CORE printer, a DLP 3D printer built to print viscous and filled photopolymers.



2

DIELECTRIC RESONATOR ANTENNAS (DRAs) AND DIELECTRIC REFLECTARRAY ANTENNA (DRA) [5]–[15]

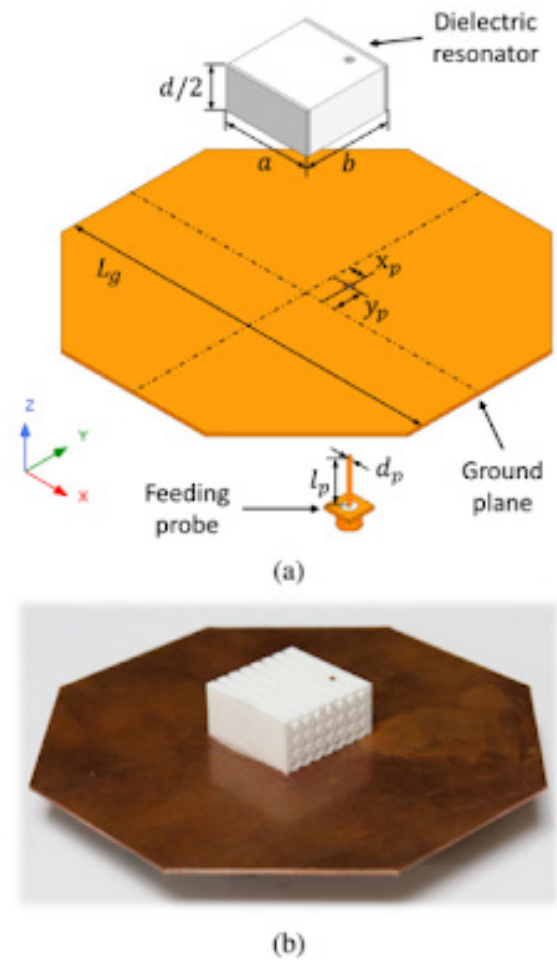
Unlike traditional metallic antennas, dielectric resonator antennas (DRAs) are formed of dielectric material, and hence do not suffer the same conduction losses and skin effect losses intrinsic to metallic radiators. DRAs are radiating dielectric resonators that transform the guided waves output from an antenna feed to unguided waves using the resonant structure of the dielectric itself. Typical patch, dipole, and monopole radiators used in antennas or antenna arrays for Microwave/mmWave applications can be designed to be compact, low weight, and relatively low-cost, but suffer from low radiation efficiency and narrow impedance bandwidth unless advanced design techniques and materials are used. DRAs are a solution to these challenges, as DRAs can be designed to exhibit good radiation efficiency and a wide impedance bandwidth even into the high mmWave frequencies.

Early DRAs were typically realized using ceramic materials, as the size and performance characteristics of DRAs are proportional to the wavelength of the resonant frequency divided by the square root of the effective relative permittivity of the dielectric material. This means that DRAs can be implemented at a fraction of the size of metallic radiator antennas, given that the dielectric constant of the material is high enough. Moreover, the loss of a DRA is directly related to the loss tangent of the dielectric material, so low-loss materials result in high radiation efficiency DRAs. As there are some low-loss dielectric materials that can operate into the hundreds of gigahertz, DRAs implemented using comparatively low relative permittivity materials can be made that exhibit desirable characteristics where metallic radiator antennas may not be viable at these high mmWave frequencies due to frequency dependent losses.

For higher operating frequencies, ceramic dielectrics are not necessary, and polymers with lower dielectric constants, such as polyvinyl chloride (PVC) have been demonstrated to realize effective DRAs. Though the size reduction benefits of having a higher relative permittivity are sacrificed somewhat with polymers compared to ceramics, very low-loss of 3D printable polymer resins can enable high efficiency DRAs with enough fabrication degrees of freedom to implement a wide range of various DRA design techniques. The freedom to implement these techniques can allow for enhanced control of key DRA performance characteristics, such as gain, bandwidth, and polarization properties.

Additionally, 3D printed DRAs can be made in such a way that the entire structure, including the feed and ground plane if a selective metallization process is used, can be realized using 3D printed technology. This can allow for integration of lenses or other antenna/antenna array features to be designed and integrated into a single manufacturing process, which may allow for improved yields, repeatability, and quality control. Many DRAs are made using high frequency laminates or sheet metal, which may not be needed with a 3D printed DRA.

A Dielectric Reflectarray antenna is essentially a hybrid design that uses a sub-wavelength grid of metastructure unit cells with variable reflection phase and individual feeds as an alternative to a traditional parabolic dish antenna. In this way the benefits of high gain achieved with parabolic antennas can be achieved with a low-profile array antenna that may also accommodate beamsteering depending on the design. Reflectarray antennas can be realized in a variety of ways, of which using planar laminates or metallized sheets with patch antenna or other planar antenna typologies and layered dielectric sheets is common. Much like with Dielectric Resonator Antennas, Dielectric Reflectarray Antennas could be fabricated using 3D printed low-loss resins, along with metallized sheets/antenna feeds. Using a unit cell that is 3D printed with high precision DLP techniques can result in highly precise and repeatable unit cells with tight control of the variable reflection phases of the array units.



(A) exploded view of the uniaxial anisotropic DRA where the grey parts of the dielectric resonator represent the isotropic zirconia walls ($a = b = 25.80$ mm, $d = 25.20$ mm, $L_g = 110.87$ mm $l_p = 12.60$ mm, $d_p = 1.23$ mm, $x_p = 5.29$ mm, and $y_p = 8.29$ mm) picture of the 3D-printed DRA **Source: [11]**

3

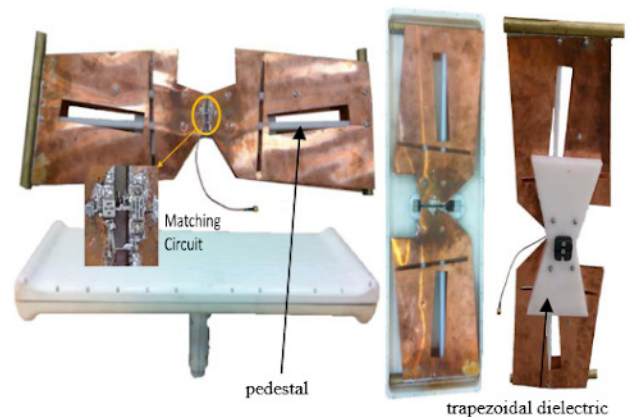
DIELECTRIC BLADE ANTENNAS [8], [10], [16]–[19]

For applications, such as unmanned aerial vehicles (UAVs), that require high performance communication and sensing technology but also aerodynamic designs, blade monopole antennas have become increasingly common. A blade monopole antenna is a modified planar monopole in the shape of an aerodynamic blade, which exceeds cylindrical monopoles in bandwidth and drag coefficient, and therefore are more desirable for UAVs and other aeronautic applications.

Due to the extreme environment in which these blade antennas are placed, they are necessarily protected from that environment with a protective dielectric shell, known as a radome. Some blade antennas are fabricated using metallized planar laminates, such as high frequency PCB materials, and hence require three design steps. The first step is the design of the antenna, and then another step is the design of the radome, and a third is to optimize the radome/blade antenna designs.

The fin, fan, or blade shape of these antennas, as well as the environmental ruggedness requirements of the radome and antenna lead to significant design constraints. This is likely why the majority of blade antennas appear to be single-element or complex dual/multiband designs in a signal blade housing, with the exception of a commercially available dual-band blade antenna array [19] that uses a two blade system with some quadrant direction finding radiation pattern capability.

The ability to 3D print low-loss dielectric structures could enable the design of more capable antenna or even antenna arrays in an aerodynamic blade shape without the limitations of traditional wide-band planar monopole designs. Moreover, it is possible, given the right materials and protective coatings, that a 3D DLP printed dielectric blade antenna could function as a dielectric antenna/antenna array and radome. Internal lattice structures, such as gradient refractive index (GRIN) lenses could further be used to enhance the gain of antenna elements within the blade to provide enhanced communication and sensing performance. With selective metallization or custom design metallic components, assembly and secondary processing of such an antenna could be minimized while enhancing repeatability and yield compared to conventional blade antennas composed of several components in which the assembly tolerances are critical.



Photographs of the fabricated antenna prototype: back, top, and bottom views. The fabricated radome and the antenna pedestal as a fixture are also shown. **Source:** [16]

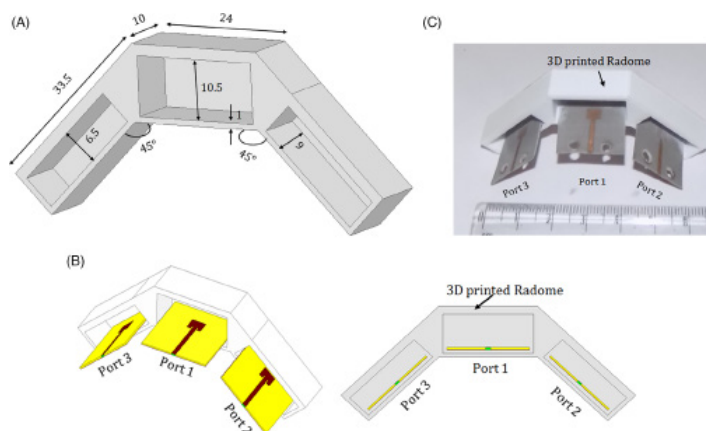
4

REPLACEMENT PROCESS FOR DIELECTRIC FOAMS IN MICROWAVE/MILLIMETER-WAVE ANTENNA AND RADOME APPLICATIONS [20]–[24]

In the case of upper microwave/mmW antenna and array antenna, dielectric foams are often used as a support structure for metallized antenna components, feeds, and as a circuit board material. These foams are made of low-loss and low-Dk dielectric material filled with air pockets to further reduce the high frequency losses and impact on the supported metallic structures. An example of the use of these engineering foams is a sandwiched lamination of a foam board with metallized multilayer laminate material patterned with capacitively coupled patch antennas on the top and bottom sides. Additional subtractive manufacturing may be used to remove any additional foam/laminate material to further drive down the effective relative permittivity and high frequency losses. Currently, there aren't any mainstream solutions for creating plated through holes with this technology, and designs are limited to planar structures or require other methods of routing signals between layers.

During lamination of these engineering foams, the foams themselves are crushed somewhat, which can be planned for and is part of the design considerations, but does add some level of error to the assembly process and creates the potential for repeatability issues. These materials must also be subtractively manufactured, typically with a mill, which adds other tolerance considerations and often substantial material waste.

A 3D DLP printing process with low-loss and low-permittivity material could be used to print either unit cells or an entire antenna/antenna array, depending on the size of the construction. Following the previous example, a 3D printed version could be printed to use minimal material, only that which is necessary to support the surfaces, feeds, and circuit structures that need to be metallized. With an adequate metallization process, such a 3D printed antenna/array can be fabricated in fewer steps with greater control of process variables. Potentially, the 3D printed hollow or lattice structure structure (with air-filled voided space) may nearly match a milled foam/laminate structure in the effective dielectric permittivity, and likely provide greater degrees of freedom. An example of this would be to 3D print an antenna/array on a curve, or fin/blade structure, which would be exceedingly complex using planar laminates and engineering foams boards.



A, Schematics of the proposed radome (units:mm). B, Schematics of the proposed radome integrated with antennas C, Photographs of the proposed antenna module **Source: [20]**



5

DIELECTRIC WAVEGUIDES FOR UPPER MILLIMETER-WAVE & THZ APPLICATIONS INCLUDING SUBSTRATE INTEGRATED WAVEGUIDE COMPONENTS [25]–[31]

There has been substantial interest over the past decade to develop terahertz (THz) communication and sensing technologies for a wide variety of applications. Technologies to roughly 100 GHz and beyond 10 THz (light) have been well developed, but there is a gap in capabilities between commonly used microwave/mmW frequencies and optical frequencies. Unlike optical transmission or sensing methods, THz technologies could have the benefits of operating through some common materials, such as wood, plastic, and fabrics. Conversely, THz technologies could enable much higher resolution sensing and higher bandwidth telecommunication capability, albeit at shorter effective ranges, than commonly used microwave/mmW technologies.

A challenge with THz technologies is that the size of structures in this frequency range scales with the wavelength. Hence, THz structures are very small in size, and a THz waveguide is on the scale of mm to micrometers. Traditional microwave/mmW conductive structures, such as metallic waveguides, are difficult or otherwise infeasible for these frequencies of operation.

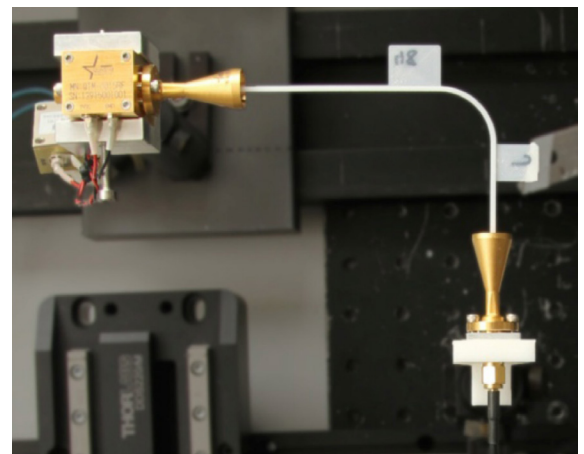
However, the unique nature of electromagnetic energy at these frequencies does allow for the use of dielectric waveguides and waveguide components. The use of dielectric waveguides is often performed for optical applications, such as visible and infrared light waveguides on semiconductor substrates. Given the relative wavelengths of THz, dielectric waveguides can be made with precision machining, such as the use of CNC milling of transparent HDPE polymers for upper microwave devices.

Top view of the experimental setup. Transceiver (upper left) and receiver have both attached a horn antenna. A waveguide is placed inside the horns (end-butt coupling) and mounted on a blade using one of the tin supports. **Source:** [26]

A caveat to this is that subtractive manufacturing of THz waveguide interconnect and components severely limits the degrees of freedom in design, often requires multiple layers or parts to be assembled, and suffers from repeatability issues. Moreover, subtractive manufacturing systems, such as CNC mills are often designed to work with metals and require special setup and expertise when machining various non-metallic materials, such as low-loss/low-dielectric constant plastics.

3D printed resin materials that are both low-loss/low-dielectric constant can be used as dielectric waveguide interconnect, components, and even entire assemblies. Waveguide components, such as splitters/combiners, attenuators, filters, and other waveguide components could be designed in the same structure as dielectric waveguide interconnect.

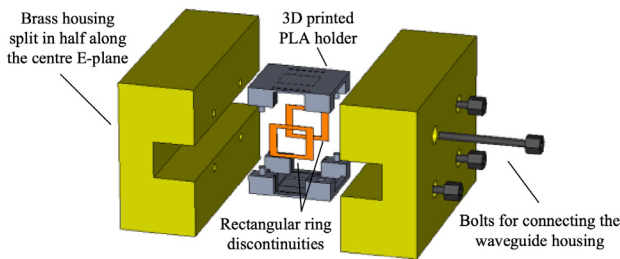
If a selective metallization process is available, it could be possible to fashion complete passive systems, including antennas/arrays using 3D printed dielectric waveguide interconnect and components. This process could further be used to fabricate substrate integrated waveguide (SIW) components and interconnection allowing for low-profile and high customizable SIW processes.



6

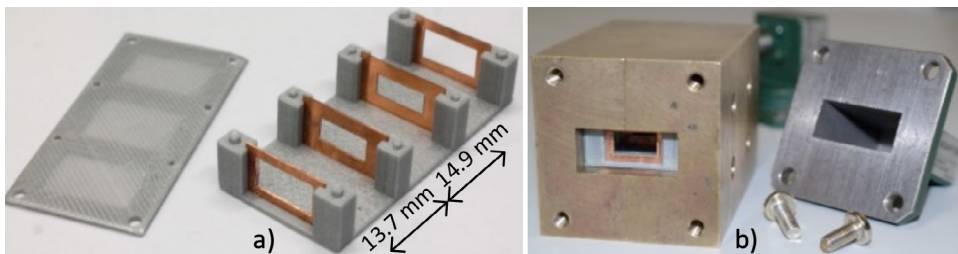
CUSTOM WAVEGUIDE AND TAILORED WAVEGUIDE PROPAGATION CHARACTERISTICS WITH DIELECTRIC LOADS INCLUDING WAVEGUIDE FILTERS [32], [27]–[31], [33]–[36]

Typical microwave/mmW waveguides are fabricated using folded and brazed/welded sheet metal with brazed/soldered flanges, extruded stock with brazed/soldered/welded flanges, or if the component or section is small/complex, machined (CNC or lathe) parts may be assembled using bolts and even precision laser welding. Given the tight tolerances and need for a smooth surface finish, waveguide interconnect and components are often plated with gold and other highly conductive and corrosion resistant coatings. Traditional waveguides are often machined from brass stock, or other engineered metals chosen for their corrosion resistance, conductivity, and machinability.



Proposed waveguide resonator: metal rings milled from a copper sheet are enclosed within a 3D printed thermoplastic holder to form an insert that can be put inside a brass waveguide housing. **Source:** [31]

As there are limitations to bending/flexing of a waveguide interconnect for complex routing, traditional subtractive machining limits the degrees of freedom of design significantly. Hence, many organizations, including NASA, where weight sensitivity, flexible design, and cost constraints are critical, are developing methods of 3D printing microwave/mmW dielectric structures that can then integrate with conductive materials or be plated to realize waveguide components and interconnects [32]. Recently available low-loss and low-dielectric constant 3D DLP resins have been demonstrated to provide enhanced microwave/mmW performance compared to other high frequency FDM filaments, polymers, and resins [1]–[4]. With surface plating or selective plating technology, complex metallic and dielectric structures could be fabricated with the new processes that aren't constrained by traditional waveguide interconnect routing limitations or internal machined waveguide cavities. With the ability to fabricate regions of varying dielectric constant based on infill, such as with gradient refractive index regions or lattice regions, waveguide interconnect, combiners/splitters, filters, and attenuators could all be made in relatively few stages. This process can enable minimized risk of misalignment, weight/material use optimization, and greater degrees of design freedom to fit in confined/complex areas compared to traditional waveguide components.



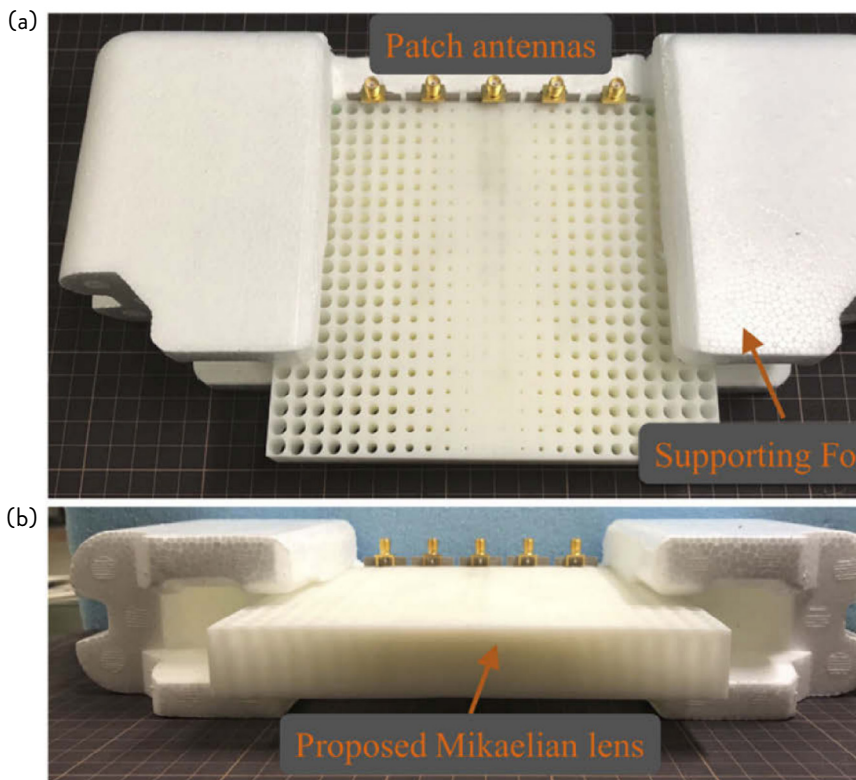
Photographic of a) 3rd order filter insert with asymmetrical holder and b) complete filter with removed waveguide to coaxial adapters. Gained texture of the bottom part of the sample is due to low infill percentage. **Source:** [31]

7

FLAT/PANEL ANTENNAS/LENSES FOR SATELLITE AND UNMANNED VEHICLE (LOW-PROFILE) & COLLAPSIBLE ANTENNA ARRAY/SYSTEM [37]-[42]

For a variety of space, ground station, satellite, and unmanned vehicle applications there is a desire to reduce the weight, size, and profile of the sensing and communications systems. These goals also coincide with the demand for more capable sensing and communications systems. This is especially true for New Space satellite applications, which are striving for both small and low-profile ground station and satellite hardware. The beamsteering capability of antenna arrays and potential for a relatively flat profile are particularly attractive for these applications compared to traditional parabolic dish or waveguide horns antennas.

However, typical planar antenna structures tend to have limited gain/directivity. The gain/directivity of these planar antennas can generally be improved using dielectric lenses. The constraints of size, weight, cost, and profile placed on dielectrics in these applications can greatly limit their value in enhancing gain/directivity. Leveraging 3D printing techniques to fabricate dielectric lenses enables more optimal use of the available volume for the lens, and 3D lattice structures (such as GRIN lenses) can result in dramatically reduced weight of dielectric material.



Photographs of the fabricated Mikaelian lens antenna prototype

- (a) Perspective view.
- (b) Front view.

Source: [41]



8

CONCLUSION

Recently available 3D DLP printable materials and technology has enabled a new realm of dielectric structures for microwave/mmW applications. With how recent these advances are and the government and military use cases, there are still few publicly disclosed uses of this technology. Given the rapid ability to iterate designs with 3D printing technology, the promise of this new way of designing and fabricating dielectrics is already starting to yield viable prototypes and even production parts in a fraction of the time needed for traditional machining and often with much more optimal capability.



RESOURCES

- [1] “Millimeter-wave Hits The Mainstream, Along With All The Challenges of High Frequency Design & Fabrication.” <https://www.microwavejournal.com/articles/36990-millimeter-wave-hits-the-mainstream-along-with-all-the-challenges-of-high-frequency-design-and-fabrication> (accessed Mar. 17, 2022).
- [2] “3D Printed Dielectric Lenses Increase Antenna Gain and Widen Beam Scanning Angle.” <https://www.microwavejournal.com/articles/36375-d-printed-dielectric-lenses-increase-antenna-gain-and-widen-beam-scanning-angle> (accessed Mar. 17, 2022).
- [3] “A Gradient Index Lens to Enable 180-Degree Field-of-View in a Phased Array System | 2022-03-06 | Microwave Journal.” <https://www.microwavejournal.com/articles/37786-a-gradient-index-lens-to-enable-180-degree-field-of-view-in-a-phased-array-system> (accessed Mar. 17, 2022).
- [4] “Radix™ Printable Dielectric - Rogers Corporation.” <https://rogerscorp.com/advanced-electronics-solutions/radix-printable-dielectric> (accessed Feb. 24, 2022).
- [5] S. Keyrouz and D. Caratelli, “Dielectric Resonator Antennas: Basic Concepts, Design Guidelines, and Recent Developments at Millimeter-Wave Frequencies,” *Int. J. Antennas Propag.*, vol. 2016, p. e6075680, Oct. 2016, doi: 10.1155/2016/6075680.
- [6] K. Pance and G. Taraschi, “Ultra-Efficient Wideband Multi-Layer Dielectric Resonator Antennas and Arrays.” <https://www.microwavejournal.com/articles/37585-kristi-pance-and-gianni-taraschi-rogers-corporation> (accessed Mar. 17, 2022).
- [7] P. Nayeri and G. Brennecka, “Wideband 3D-Printed Dielectric Resonator Antennas,” in 2018 IEEE International Symposium on Antennas and Propagation USNC/URSI National Radio Science Meeting, Jul. 2018, pp. 2081–2082. doi: 10.1109/APUSNCURSINRSM.2018.8608331.
- [8] G. Varshney, V. S. Pandey, and R. S. Yaduvanshi, “Dual-band fan-blade-shaped circularly polarised dielectric resonator antenna,” *IET Microw. Antennas Propag.*, vol. 11, no. 13, pp. 1868–1871, 2017, doi: 10.1049/iet-map.2017.0244.
- [9] F. P. Chietera, R. Colella, and L. Catarinucci, “Dielectric Resonators Antennas Potential Unleashed by 3D Printing Technology: A Practical Application in the IoT Framework,” *Electronics*, vol. 11, no. 1, Art. no. 1, Jan. 2022, doi: 10.3390/electronics11010064.
- [10] Q. Wu, “Design of a broadband blade and DRA hybrid antenna with hemi-spherical coverage for wireless communications of UAV swarms,” *AEU - Int. J. Electron. Commun.*, vol. 140, p. 153930, Oct. 2021, doi: 10.1016/j.aeue.2021.153930.
- [11] C. D. Morales Peña, C. Morlaas, A. Chabory, R. Pascaud, M. Grzeskowiak, and G. Mazingue, “3D-printed ceramics with engineered anisotropy for dielectric resonator antenna applications,” *Electron. Lett.*, May 2021, Accessed: Feb. 24, 2022. [Online]. Available: <https://hal.archives-ouvertes.fr/hal-03231596>
- [12] Z.-X. Xia, K. W. Leung, and K. Lu, “3-D-Printed Wideband Multi-Ring Dielectric Resonator Antenna,” *IEEE Antennas Wirel. Propag. Lett.*, vol. 18, no. 10, pp. 2110–2114, Oct. 2019, doi: 10.1109/LAWP.2019.2938009.



RESOURCES

- [13] B. Huang, Q. Qiang, and G. Vandenbosch, “High Power Dielectric Reflectarray Antenna using 3D Printing Technology,” undefined, 2019, Accessed: Mar. 21, 2022. [Online]. Available: <https://www.semanticscholar.org/paper/High-Power-Dielectric-Reflectarray-Antenna-using-3D-Huang-Qiang/d9cc935da76cba83f9785508f0d6b5ef31904802>
- [14] P. Nayeri et al., “High gain dielectric reflectarray antennas for THz applications,” in 2013 IEEE Antennas and Propagation Society International Symposium (APSURSI), Orlando, FL, USA, Jul. 2013, pp. 1124–1125. doi: 10.1109/APS.2013.6711222.
- [15] L. Guo, S. Li, X. Liao, X. Jiang, and L. Peng, “Wideband 3D-printed dielectric reflectarray in Ka-band,” *Microw. Opt. Technol. Lett.*, vol. n/a, no. n/a, doi: 10.1002/mop.33170.
- [16] M. Nosrati, A. Jafarholi, R. Pazoki, and N. Tavassolian, “Broadband Slotted Blade Dipole Antenna for Airborne UAV Applications,” *IEEE Trans. Antennas Propag.*, vol. 66, no. 8, pp. 3857–3864, Aug. 2018, doi: 10.1109/TAP.2018.2835524.
- [17] W. F. Silva, I. Bianchi, and T. P. Santos, “Design of a Blade Antenna Embedded in Low-Cost Dielectric Substrate,” *J. Microw. Optoelectron. Electromagn. Appl.*, vol. 16, pp. 180–193, Mar. 2017, doi: 10.1590/2179-10742017v16i1881.
- [18] T. Rahim, A. Wahab, and J. Xu, “Open ended dielectric filled slot blade antenna design with coaxial feed for airborne applications,” in IET International Radar Conference 2015, Oct. 2015, pp. 1–3. doi: 10.1049/cp.2015.0968.
- [19] “Blade-Antenna-System.pdf.” Accessed: Mar. 21, 2022. [Online]. Available: <https://etiworld.com/wp-content/uploads/2021/07/Blade-Antenna-System.pdf>
- [20] G. S. Karthikeya, S. K. Koul, A. K. Poddar, and U. Rohde, “Path loss compensated millimeter wave antenna module integrated with 3D-printed radome,” *Int. J. RF Microw. Comput.-Aided Eng.*, vol. 30, no. 10, p. e22347, 2020, doi: 10.1002/mmce.22347.
- [21] J.-K. Che and C.-C. Chen, “Wideband axial-mode helical antenna with 3D printed proliferated radome,” in 2017 IEEE International Symposium on Antennas and Propagation USNC/URSI National Radio Science Meeting, Jul. 2017, pp. 695–696. doi: 10.1109/APUSNCURSINRSM.2017.8072390.
- [22] “ROHACELL® in antennas and electronics - Evonik Industries.” <https://www.rohacell.com/en/markets/antennas-and-electronics> (accessed Feb. 24, 2022).
- [23] “ROHACELL® - Evonik Industries.” <https://composites.evonik.com/en/products-services/foams/rohacell> (accessed Mar. 21, 2022).
- [24] “AIREX high performance foam core material | 3A.” <https://www.3accorematerials.com/en/markets-and-products/airex-foam> (accessed Mar. 21, 2022).
- [25] D. Jahn et al., “3D printed chirped dielectric waveguide for focusing applications,” in 2016 41st International Conference on Infrared, Millimeter, and Terahertz waves (IRMMW-THz), Sep. 2016, pp. 1–2. doi: 10.1109/IRMMW-THz.2016.7758656.



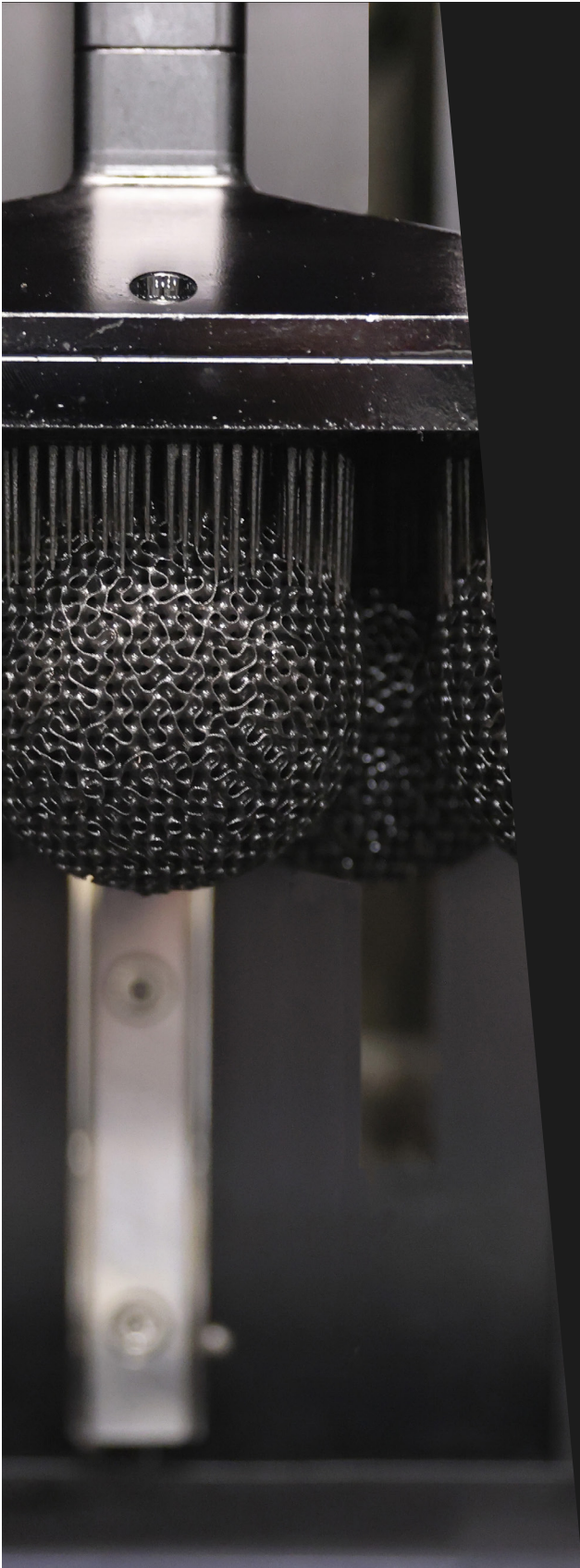
RESOURCES

- [26] M. Weidenbach et al., “3D printed dielectric rectangular waveguides, splitters and couplers for 120 GHz,” *Opt. Express*, vol. 24, no. 25, pp. 28968–28976, Dec. 2016, doi: 10.1364/OE.24.028968.
- [27] C. Tomassoni, R. Bahr, M. Tentzeris, M. Bozzi, and L. Perregri, “3D printed substrate integrated waveguide filters with locally controlled dielectric permittivity,” in 2016 46th European Microwave Conference (EuMC), London, United Kingdom, Oct. 2016, pp. 253–256. doi: 10.1109/EuMC.2016.7824326.
- [28] E. Massoni et al., “3D printing and metalization methodology for high dielectric resonator waveguide microwave filters,” in 2017 IEEE MTT-S International Microwave Workshop Series on Advanced Materials and Processes for RF and THz Applications (IMWS-AMP), Pavia, Sep. 2017, pp. 1–3. doi: 10.1109/IMWS-AMP.2017.8247417.
- [29] E. Massoni et al., “Characterization of 3D-printed dielectric substrates with different infill for microwave applications,” in 2016 IEEE MTT-S International Microwave Workshop Series on Advanced Materials and Processes for RF and THz Applications (IMWS-AMP), Jul. 2016, pp. 1–4. doi: 10.1109/IMWS-AMP.2016.7588330.
- [30] Y. Kim and S. Lim, “Low Loss Substrate-Integrated Waveguide Using 3D-Printed Non-Uniform Honeycomb-Shaped Material,” *IEEE Access*, vol. 8, pp. 191090–191099, 2020, doi: 10.1109/ACCESS.2020.3032132.
- [31] U. Jankovic, N. Mohottige, A. Basu, and D. Budimir, “Low-Cost Hybrid Manufactured Waveguide Bandpass Filters with 3D Printed Insert Dielectric,” in 2019 49th European Microwave Conference (EuMC), Oct. 2019, pp. 316–319. doi: 10.23919/EuMC.2019.8910933.
- [32] C. M. Shemelya et al., “3D Printing Multi-Functionality: Embedded RF Antennas and Components,” presented at the European Conference on Antennas and Propagation, Lisbon, Apr. 2015. Accessed: Mar. 22, 2022. [Online]. Available: <https://ntrs.nasa.gov/citations/20150006817>
- [33] V. Kesari, *Metal- and Dielectric-Loaded Waveguide: An Artificial Material for Tailoring the Waveguide Propagation Characteristics*. IntechOpen, 2019. doi: 10.5772/intechopen.82124.
- [34] K. Y. Chan, R. Ramer, and R. Sorrentino, “Low-Cost Ku-Band Waveguide Devices Using 3-D Printing and Liquid Metal Filling,” *IEEE Trans. Microw. Theory Tech.*, vol. 66, no. 9, pp. 3993–4001, Sep. 2018, doi: 10.1109/TMTT.2018.2851573.
- [35] H. Aghayari, J. Nourinia, C. Ghobadi, and B. Mohammadi, “Realization of dielectric loaded waveguide filter with substrate integrated waveguide technique based on incorporation of two substrates with different relative permittivity,” *AEU - Int. J. Electron. Commun.*, vol. 86, pp. 17–24, Mar. 2018, doi: 10.1016/j.aue.2018.01.008.
- [36] “Providing flexibility - HUBER+SUHNER.” <https://www.hubersuhner.com/en/solutions/rf-energy/providing-flexibility> (accessed Mar. 22, 2022).
- [37] Q.-W. Lin and H. Wong, “A Low-Profile and Wideband Lens Antenna Based on High-Refractive-Index Metasurface,” *IEEE Trans. Antennas Propag.*, vol. 66, no. 11, pp. 5764–5772, Nov. 2018, doi: 10.1109/TAP.2018.2866528.



RESOURCES

- [38] A. Papathanasopoulos, Y. Rahmat-Samii, N. C. Garcia, and J. D. Chisum, “A Novel Collapsible Flat-Layered Metamaterial Gradient-Refractive-Index Lens Antenna,” *IEEE Trans. Antennas Propag.*, vol. 68, no. 3, pp. 1312–1321, Mar. 2020, doi: 10.1109/TAP.2019.2944546.
- [39] H. Eskandari, J. L. Albadalejo-Lijarcio, O. Zetterstrom, T. Tyc, and O. Quevedo-Teruel, “H-plane horn antenna with enhanced directivity using conformal transformation optics,” *Sci. Rep.*, vol. 11, no. 1, p. 14322, Jul. 2021, doi: 10.1038/s41598-021-93812-6.
- [40] S. Paul and M. J. Akhtar, “Novel Metasurface Lens-Based RF Sensor Structure for SAR Microwave Imaging of Layered Media,” *IEEE Sens. J.*, vol. 21, no. 16, pp. 17827–17837, Aug. 2021, doi: 10.1109/JSEN.2021.3084614.
- [41] W. Shao and Q. Chen, “Performance analysis of an all-dielectric planar Mikaelian lens antenna for 1-D beam-steering application,” *Opt. Express*, vol. 29, no. 18, pp. 29202–29214, Aug. 2021, doi: 10.1364/OE.438182.
- [42] F. Fan, M. Cai, J. Zhang, Z. Yan, and J. Wu, “Wideband Low-Profile Luneburg Lens Based on a Glide-Symmetric Metasurface,” *IEEE Access*, vol. 8, pp. 85698–85705, 2020, doi: 10.1109/ACCESS.2020.2992653.



WWW.3DFORTIFY.COM
SALES@3DFORTIFY.COM
75 HOOD PARK DRIVE, BLDG 510, BOSTON, MA 02129